Petroleum Science 20 (2023) 1005–1017

Contents lists available at ScienceDirect

Petroleum Science

journal homepage: www.keaipublishing.com/en/journals/petroleum-science

Original Paper

# Unlocking the potentials of gel conformance for water shutoff in fractured reservoirs: Favorable attributes of the double network gel for enhancing oil recovery

Qian-Hui Wu [a, b], Ji-Jiang Ge [a, *], Lei Ding [c], Gui-Cai Zhang [a]

[a] School of Petroleum Engineering, China University of Petroleum (East China), Qingdao, 266580, Shandong, PR China
[b] Laboratoire Sciences et Ingénierie de la Matière Molle, ESPCI Paris, PSL University, 75005, Paris, France
[c] Total Energies SE., E&P, Pôle d'Etudes et Recherche de Lacq, BP 47, LACQ, 64170, France

ARTICLE INFO

*Article history:*
Received 25 April 2022
Received in revised form
18 October 2022
Accepted 25 October 2022
Available online 29 October 2022

Edited by Yan-Hua Sun

*Keywords:*
Double network structure
Gel swelling
Rupture pressure
Fractured core
Oil recovery factor

ABSTRACT

The double-network prepared with an *in-situ* monomer gel and a fast-crosslinked Cr(III) gel is introduced to develop a thixotropic and high-strength gel (THSG), which is found to have many advantages over the traditional gels. The THSG gel demonstrates remarkable thermal stability, and no syneresis is observed after 12 months with high salinity brine (95,500 mg/L). Moreover, the SEM and XRD results indicate that the gel is intercalated into the lamellar structures of Na-MMT, where the gel can form a uniform and compact structure. In addition, the THSG gel has an excellent swelling behavior, even in the high salinity brine. In the slim tube experiments, the THSG gel exhibits high rupture pressure and improves blocking capacity after being ruptured. The core flooding results show that a layer of gel filter cake is formed on the face of the fracture, which may be promoted by a high matrix permeability, a small aperture fracture, and a high injection rate. After the gel treatment, the fracture can be completely blocked by the THSG gel. It is found that a high incremental oil recovery (65.3%) can be achieved when the fracture was completely blocked, compared to 40.2% if the gel is ruptured. Although the swelling of ruptured gel can improve oil recovery, part of the injected brine may be channeled through the gel-filled fractures, resulting in a decrease in the sweep efficiency. Therefore, the improved blocking ability by gel swelling (e.g., in fresh water) may be less efficient to contribute to an enhancement of oil recovery. It is also found that the pressure gradient and residual resistance factor to water ($F_{rrw}$) are higher if the matrix is less permeable, indicating that the fractured reservoir with lower matrix permeability may require a higher gel strength for treatment. The findings of this study may provide novel insights on designing robust double network gels for water shutoff in fractured reservoirs.


## 1. Introduction

The oil recovery in fractured sandstone reservoirs is typically low due to the unfavorable water channeling issues. Polymer gels are usually applied for water-shutoff in fractured reservoirs, which have been proven to be economically feasible to alleviate the adverse effect of the heterogeneity of the fractured reservoir and efficiently improve the sweep efficiency of the chase-floods (Demir et al., 2008; Zhang and Bai, 2011; Imqam and Bai, 2015; Canbolat and Parlaktuna, 2019; Wu et al., 2021, 2022).

A successful polymer gel treatment mainly depends on the rupture pressure of the gel system (Ganguly et al., 2002; Brattekås et al., 2016; Seright and Brattekås, 2021; Zhang et al., 2021). Previously, Sydansk et al. (2004) evaluated the mechanical strength and performance of gels formulated with a combination of high-molecular-weight and low-molecular-weight polymers. The results showed that brine started breakthrough from the gel in a 1 mm aperture fracture when the pressure gradient was 2 MPa/m (88 psi/ft). Comparatively, the rupture pressure gradient of gel was decreased to 0.84 MPa/m (37 psi/ft) and 0.57 MPa/m (25 psi/ft), when the fracture aperture was increased to 2 and 4 mm, respectively. Provided that the imposed pressure exceeds the gel rupture pressure, the fluid would penetrate through the gel and generate

* Corresponding author.
*E-mail address:* gejijiang@163.com (J.-J. Ge).

https://doi.org/10.1016/j.petsci.2022.10.018

certain new flow paths in the gel-filled fractures, which allow the chase fluid flowing through these narrow paths.

The *in-situ* gel systems, such as the organically crosslinked polymer gels and monomer polymerized gels, have more robust and flexible structures, which can substantially improve the gel strength and enable the gel to withstand high pressure gradients during chase brine injection (El-Karsani et al., 2015; Chen et al., 2019; Kang et al., 2021; Wu et al., 2022). However, one challenge is that the gelant may be leaked off into the adjacent matrix during the gel placement. Although the gel formed within the matrix (by the leaked-off gelant) may provide a higher flow resistance, it would also significantly reduce the permeability of the matrix, especially under oil-wet conditions (Ganguly et al., 2002; Khamees and Flori, 2018).

It is reported that using partially formed polymer gel (PFPG) can effectively limit the extrusion of gel into the matrix. Since the mature gel has a sufficiently robust gel structure, it would not be substantially penetrated into the adjacent matrix (Seright, 2003; Sydansk et al., 2005; Brattekås et al., 2015, 2016). However, the blocking ability of these gels is generally poor, thus providing little resistance to the chase floods, especially when the permeability contrast between the fractures and the matrix is large (Brattekås and Seright, 2018). Previous results have shown that the pressure gradient causing the gel failure was almost the same as that for gel to be extruded through the fracture (Seright, 2003). In addition, the effect of the gel state during gel treatment was summarized by Brattekås et al. (2015). The results indicated that the mature gel demonstrated a higher rupture pressure than the immature gel (gelant), and the rupture pressure of a majority of the mature gels was approximately 0.34 MPa/m (15 psi/ft). The formed gel may be dehydrated during its extrusion through a fracture, resulting in a more concentrated gel. This would be beneficial for enhancing the blocking ability of the gel during chase floods. For the immature gel, the gelant normally formed a less concentrated gel due to dispersion of the crosslinkers, which, therefore, could be easily displaced from the fractures during the chase brine injection (Ganguly et al., 2002; Wilton and Asghari, 2007; Seright and Brattekås, 2021). Consequently, the poor blocking ability has impeded the use of these weak gel systems for water shutoff in large aperture fractures.

Previous studies have shown that double network (DN) is one of the most effective methods to enhance the gel strength as well as mitigate the leakoff of the gelant (Zhang et al., 2009; Gong, 2010; Jia et al., 2011; Du et al., 2019). The DN gels typically consist of two highly asymmetrically crosslinked networks: a tightly crosslinked network with monomer and a loosely crosslinked network with polyacrylamide (Xin et al., 2013; Krakovský et al., 2019). The first tightly crosslinked network is the major component and has a significant effect on the strength of DN gel. It can be an organically crosslinked polymer gel or a monomer polymerized gel. The second network, designed to reinforce the first (tightly crosslinked) network, is generally a weak and fast-crosslinking polymer gel system, which plays an important role in stabilizing the structure of the tight gel system (Jia et al., 2011). The fast-crosslinking gel may be gelated during DN gel placement in fractures, which would consequently limit the components of tight network gel from leaking into the matrix (Du et al., 2019). It is also reported that the strength of gel can be greatly enhanced by adding clays (Filippone et al., 2008; Haque et al., 2012).

The salinity of injection water and the salinity of gel solvent have significant impacts on the gel performance (Zhang and Bai, 2011; Lenji et al., 2018; Alhuraishawy et al., 2018; Khamees and Flori, 2018; Brattekås et al., 2016). Recent studies have shown that the gel prepared with higher salinity brine exhibited larger water permeability reduction and higher oil recovery (Zhang and Bai, 2011; Brattekås and Seright, 2018). The gel may be swollen and re-block the flow paths even after it has been ruptured, thereby improving its blocking capacity. This phenomenon would occur when the salinity of the injected water is lower than the salinity of the gel solvent (Seright and Brattekås, 2021). The swelling ratios of the gels are usually decreased with increasing the salinity of injection brine. Contrarily, the gels would shrink when the salinity of surrounding brine is higher than the salinity of the gel solvent (Tu and Wisup, 2011; Jamali et al., 2020; Mahon et al., 2020; Guo et al., 2022). However, the gel prepared with high salinity water would result in notable decreases in the gel strength and its long-term stability (El-Karsani et al., 2015; Wang et al., 2016). Moreover, most of the swollen gels may become too weak and brittle to sustain the imposed pressure (Wang et al., 2012).

In this study, we developed a double-network gel system and evaluated its potential for blocking the large aperture fractures. In order to mitigate the leak-off of the gelant into the matrix, a fast-crosslinking gel was introduced into the gel system, which is composed of 0.2 wt% HPAM and 0.0125 wt% chromium acetate (Cr(III)). The clay particles were also introduced into the gel system, which endowed the THSG solution a good thixotropic property and the THSG a good swelling ability. Previously, the rheological properties of the THSG solution and the propagation of the gelant in parallel-plate fractured models as well as in slim tubes have been systematically investigated (Ge et al., 2022). In this study, we focused on evaluating the potential of the THSG with high rupture pressure for water shutoff in model fractures in porous media, which could largely contribute to the success of gel treatment in large aperture fractures generated by hydraulic fracturing. The properties of *in-situ* monomer polymerization gel (IMPG) and the fast-crosslinking gel system were studied, and the strengthen mechanisms of the clay particles were investigated by XRD and SEM measurements. The gel swelling behavior in brine of various salinity was investigated, and the effect of swelling on gel performance was discussed. Moreover, the rupture pressure of the gel in different tubes was measured to determine the blocking capacity of the gel. Finally, core flooding experiments were conducted to evaluate the gel performance in fractured cores, including the gelant injectivity, blocking capacity, and oil recovery improvement.

## 2. Experimental

### 2.1. Materials

***THSG.*** The THSG was formulated by incorporating two asymmetrically crosslinked network: a tightly crosslinked network of IMPG, and a loosely crosslinked network of fast-crosslinking polymer gel. The IMPG was prepared by acrylamide (AM), *N*,*N*′-methylene-bis-acrylamide (MBA), 4,4′-azobis (4-cynovaleric acid) (V501), and a retarder, i.e., the potassium ferricyanide (PF). V501 is a water-soluble azo initiator. The fast-crosslinking polymer gel is composed of 0.2 wt% partially hydrolyzed polyacrylamide (HPAM) and 0.0125 wt% chromium acetate (Cr (III)). The HPAM has a molecular weight of $13 \times 10^6$–$15 \times 10^6$ Da and 20%–25% degree of hydrolysis, which is supplied by Jucheng Fine Chemicals Co. (China, Anhui). Chromium (III) acetate (12.5 wt% aqueous solution) was prepared by diluting the commercial solution (50 wt%) with distilled water. The clay used in this study is sodium-based bentonite, and the purity of montmorillonite is 80%–100% (Na-MMT, from Halliburton Baroid).

***Brine.*** The total dissolved solids (TDS) of brine were 95,500 mg/L, and its composition is listed in Table 1. The brine was diluted to 1/5 of its original salinity for preparing the gels. The swelling behavior of the gel was studied in freshwater and different brine (1/3, 2/3 and 3/3 of its original salinity).

***Oil.*** The mineral oil was employed for fractured core flooding

**Table 1**
Chemical composition of the brine.

| Ion concentration, mg/L | | | | | | TDS, mg/L |
|---|---|---|---|---|---|---|
| $Na^+$ | $Ca^{2+}$ | $Mg^{2+}$ | $Cl^-$ | $SO_4^{2-}$ | $HCO_3^-$ | |
| 22092 | 8762 | 680 | 63524 | 260 | 182 | 95500 |

tests, and the properties of the oil are shown in Table 2.

### 2.2. Gelation performance

Bottle tests were applied to qualitatively determine the gelation time and strength of the gel, which were also used to examine the stability of the gel system. In these tests, the gelation time of the gel is defined as the elapsed time when the gel sample does not flow downward upon inversion of the bottle. The gel samples were placed in the water bath at constant temperature, and their strength and syneresis were examined regularly. In order to investigate the effect of the fast-crosslinking gel on gelation time, the viscosity of the samples at different time was measured at 60 °C. The shear rate was 10 $s^{-1}$.

The elastic modulus ($G'$) of the gel was determined by a rheometer (Antor Paar MCR 92) equipped with a parallel plate geometry (the diameter is 25 mm, and the gap is 1 mm). These measurements were conducted at 25 °C. The applied strain was in the range from 0.1% to 200%, and the frequency was fixed at 1 Hz.

### 2.3. Scanning electron microscopy (SEM) and X-ray diffraction (XRD) measurements

The microstructure of gel was investigated by SEM equipped with a Quorum PP3010T Cryo-SEM preparation system. Cryo-SEM allows imaging of gel samples in a frozen state. These measurements were conducted at 5 kV accelerating voltage and 5–10 mm working distance.

XRD (X′ Pert Pro MPD, Holland Panalytical) was used to identify the interplanar spacing ($d$) of clays at different conditions. The diffraction angle ($2\theta$) was recorded in the range of 0°–167°. The diffraction angles of clay particles, gelant with clay samples and the gel with clay samples were measured, and then the Bragg's Law (Eq. (1)) was used to calculate the interplanar spacing (diffraction analysis).

$$2d\sin\theta = n\lambda \tag{1}$$

where $\theta$ is the included angle between the X-ray and the corresponding crystal plane; $\lambda$ is the wavelength; $n$ is the diffraction series. The value of $n$ is taken as 1 in this study.

### 2.4. Gel swelling measurement

As discussed before, the gels were prepared with 19100 mg/L TDS brine, which was diluted from the synthetic formation brine (95,500 mg/L). The swelling ratio of the THSG was measured by the gravimetric method (Lenji et al., 2018). After being aged at 60 °C for 2 days, the gels were fetched from the ampoule, and the weight of the initial gel samples ($W_i$) was measured. Then, the gel samples were soaked in different brine at 60 °C for several months. The weight of the swollen gel was recorded as $W_s$, and the swelling ratio ($R_s$) was calculated by Eq. (2).

$$R_s = \frac{W_s - W_i}{W_i} \tag{2}$$

**Table 2**
The properties of mineral oil.

| API gravity, ° | Density (20 °C), g/cm$^3$ | Viscosity (40 °C), mPa·s | Viscosity (60 °C), mPa·s |
|---|---|---|---|
| 38 | 0.834 | 12 | 3.8 |

### 2.5. Rupture pressure

Stainless steel tubes were utilized to investigate the rupture pressure of the gels. The lengths of tubes are all 0.5 m, while the diameters are varying (1, 2, 3, and 4 mm, respectively). The gelant was firstly injected into the tubes, then the tubes were sealed and aged in an oven at 60 °C for 5 days. After then, brine was injected to impose a pressure gradient across the gel-filled tubes and to determinate the blocking ability of the gels. The injection rate was 1 mL/min.

### 2.6. Core flood experiments

The experimental set-up is a typical one for fractured core flooding studies, as shown in Fig. 1. It consists of an injection pump, three transfer vessels, a core holder, a differential pressure transducer, pressure gauges, back pressure regulators and a temperature control system. The pressure data were collected by a data acquisition system connected to a computer. All the core flood experiments were performed at 60 °C.

The core flooding tests were conducted to evaluate the gelant injection pressure, blocking ability of the gel, matrix damage, and oil recovery factor. The procedures are illustrated in the following.

***Fractured core preparation.*** The core plugs are homogeneous sandstones (Berea and Bentheimer) and low permeability carbonates (Indiana limestone) from the outcrops, which were used to study the placement of gelant and blocking ability of gel in fractured core plugs. The pore volume of the core sample was measured based on mass balance, and the initial permeability was measured by 1.5 wt% NaCl brine. Subsequently, the core sample was dried in an oven before splitting lengthwise into two pieces. The cutting surfaces were smoothed before the core was remounted into the core holder, as shown in Fig. 2. The copper wires were used to control the fracture width. The detailed properties of the core samples are shown in Table 3.

***Oil saturation.*** Firstly, the fracture of the core was blocked by a soft silicone pad and the confining pressure was cautiously controlled such that the permeability was the same as the initial permeability without the fracture. In this study, the confining pressure was kept at 3.5 MPa greater than the injection pressure. Secondly, the core sample was vacuumed, and oil was injected into the core at a rate of 2.0 mL/min. Thirdly, the core was dismounted from the core holder, the silicone pad was then removed from the fracture, and the copper wires were once again placed in the fracture to control the fracture width. Fourthly, the core was reassembled into the core holder, and oil was injected again to saturate

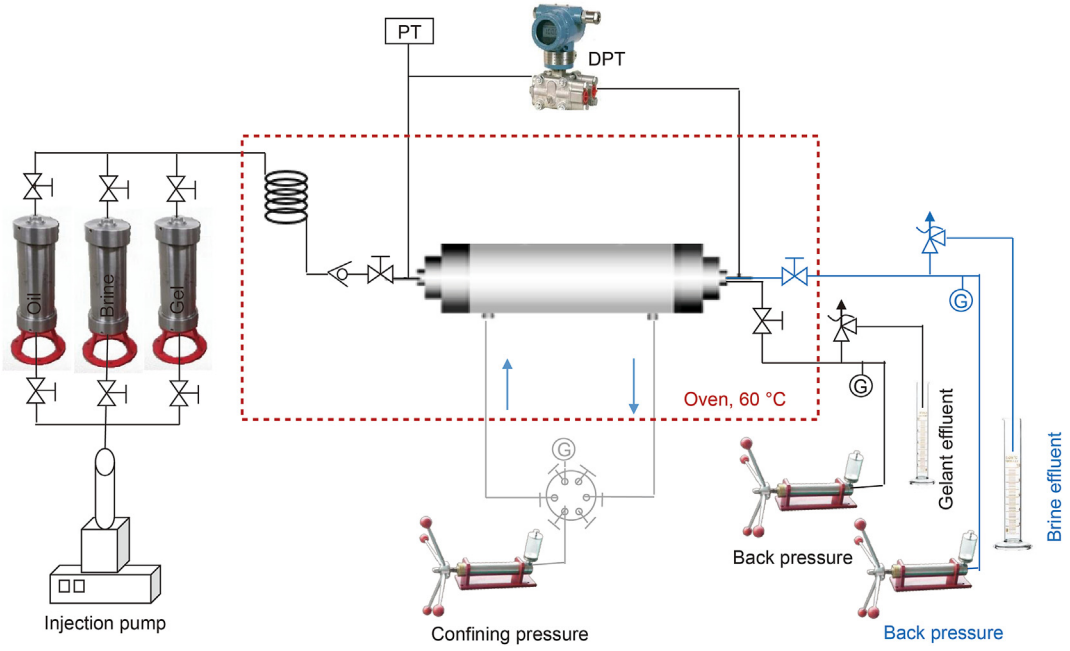


**Fig. 1.** Schematic of equipment for core flooding experiments (with vertical fractures).

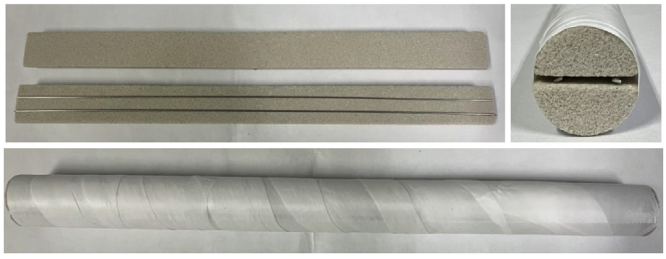

**Fig. 2.** Fractured core samples.

the fractures and compensate the loss of oil in the matrix. The core was aged for 2 days before waterflooding. The initial oil saturation for core O-1 and O-2 is assumed to be 100%.

***First water floods.*** Brine was firstly injected into the fractured core at 1 mL/min to displace the oil until no oil was produced. The salinity of the brine was the same as that prepared for the gel solvent.

***Gelant placement.*** After waterflooding, the gelant was injected into the fractured core at 1 mL/min. After then, the core was shut-in at 60 °C for several days to allow the gelation. The gelant was immediately removed from the flow lines before the curing process.

***Chase water floods.*** After gelation, brine was injected into the fractured core at 1 mL/min to evaluate the blocking ability of gel and the oil recovery factor.

***Matrix damage tests.*** The matrix permeability was measured before and after the gel treatment. After the gel treatment, the fractured core sample was unloaded from the core holder and the gel was removed from the fracture. Then, the fracture of the core was re-blocked by a soft silicone pad, and the core was remounted into the core holder to measure the permeability of the matrix. The matrix damage was characterized by $R_m$ based on Eq. (3).

$$R_m = \frac{k_i}{k_d} \times 100\% \tag{3}$$

where $k_i$ is the initial matrix permeability; $k_d$ is the permeability after gel treatment.

**Table 3**
Properties of the core samples used in this study.

| Core No. | Core type | Length, cm | Diameter, cm | Porosity $\phi$, % | Permeability $k_{matrix}$, mD | Fracture aperture, mm | Injection rate, mL/min |
|---|---|---|---|---|---|---|---|
| M-1 | Limestone | 30.1 | 2.52 | 14.8 | 11 | 2 | 1 |
| M-2 | Berea | 30.2 | 2.52 | 19.5 | 84 | 2 | 1 |
| M-3 | Bentheimer | 30.05 | 2.53 | 24.3 | 1860 | 2 | 1 |
| I-1 (M-2) | Berea | 30.2 | 2.52 | 19.5 | 84 | 2 | 1 |
| I-2 | Berea | 30.1 | 2.51 | 20.1 | 85 | 2 | 2 |
| I-3 | Berea | 30.05 | 2.52 | 20.3 | 88 | 2 | 4 |
| A-1 | Berea | 30.1 | 2.5 | 21.1 | 92 | 0.5 | 1 |
| A-2 | Berea | 30.15 | 2.51 | 19.8 | 86 | 1 | 1 |
| A-3 (M-2) | Berea | 30.2 | 2.52 | 19.5 | 84 | 2 | 1 |
| A-4 | Berea | 30.1 | 2.51 | 20.2 | 90 | 3 | 1 |
| O-1 | Berea | 30.2 | 2.52 | 20.6 | 87 | 2 | 1 |
| O-2 | Berea | 30.3 | 2.52 | 20.4 | 91 | 2 | 1 |

## 3. Results and discussion

### 3.1. Formulation of THSG

#### 3.1.1. Gelation performance of IMPG

The components of IMPG include a monomer (acrylamide), an initiator, a crosslinker, and a retarder (an agent to control the gelation time). The results have shown that the azo initiators have many advantages over other initiators (Lowe and McCormick, 2007; Yang et al., 2010). Various water-soluble azo initiators with 10-h half-life in water at a temperature range from 44 to 88 °C are commercially available (Eoff et al., 2001; Yang et al., 2010). In this study, the 4,4′-azobis (4-cynovaleric acid) (V501), a water-soluble azo initiator with a half-life temperature of 69 °C, was applied. An excess amount of initiator would increase the chain termination reactions, leading to polymerization of low molecular weight polymers. Thus, the concentration of initiator was controlled at less than 0.1 wt%. The crosslinker (MBA) can provide more crosslinking sites for the gel to form a 3-D network structure. In this study, the concentration of MBA is 0.1 wt%.

Due to the short gelation time, the application of *in-situ* monomer gels for water shutoff is limited in the reservoirs. Moreover, the initiation of polymerization is very sensitive to elevated temperatures, which would limit its placement into the target regions. When the temperature is slightly high, the reaction rate would be significantly enhanced. However, it is found that potassium ferricyanide (PF) is an effective retarder to slow down the polymerization. Since the variable valence metal salt would undergo electron transfer reaction with free radicals, some active free-radicals would be deactivated, thereby slowing down the rate of polymerization. Varying the amount of the PF can easily and accurately regulate the gelation time from a few hours to a much longer time. The results in Fig. 3 show that the gelation time of IMPG can be effectively controlled by adjusting the amount of the PF, and the gelation time can be increased up to 48 h at 60 °C. However, the IMPG, which is usually composed of unitary networks between short chain polymers, is very brittle, as shown in Fig. 4a. The brittleness of the gel may lead to a low blocking ability in fractures. Moreover, it is found that adding the large-molecular polymers can effectively improve the toughness of the gel, and the results are shown in Section 3.1.2.

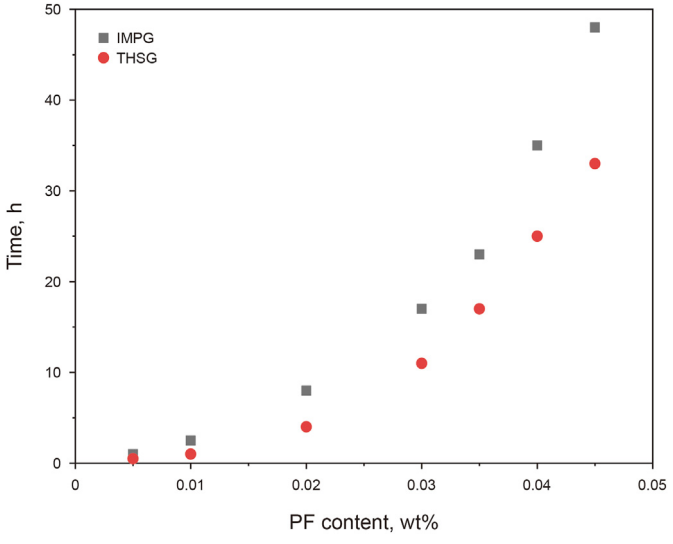


**Fig. 3.** Effect of PF content on the gelation time of IMPG and THSG at 60 °C, the formulation of the IMPG is composed of 5 wt% AM, 0.05 wt% V501, and 0.1 wt% MBA.

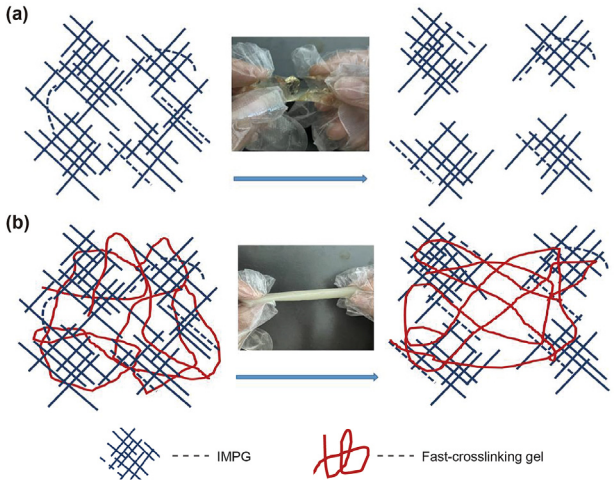


**Fig. 4.** The schematic of gel network: (**a**) single network of IMPG; (**b**) double network of THSG.

#### 3.1.2. Effect of fast-crosslinking gel system

The fast-crosslinking gel system (also known as a weak gel system) was introduced into the THSG system, and the former is composed of 0.2 wt% HPAM and 0.0125 wt% chromium acetate (Cr (III)). Moreover, Na-MMT particles were added to enhance the strength of the gel. The Na-MMT can be well compatible with 1/5 (salinity) brine. The viscosity of the gelant during gelation is shown in Fig. 5a. It can be seen that the viscosity was initially increased due to the gelation of fast crosslinking gel system in THSG. The results also show that the THSG gel strengthened with the weak gel system and 1.5 wt% clay particles exhibits high gel strength and long-term gel stability. The elastic modulus of gel samples is shown in Fig. 5b. The storage modulus ($G'$) of gel was increased from 86 Pa (IMPG) to about 240 Pa (THSG), after the samples were aged for 5 days. Actually, the high-strength gels have been widely reported in the literature (Al-Muntasheri et al., 2008; El-Karsani et al., 2015). It was reported that the $G'$ for the polyacrylamide/polyethyleneimine ((PAM/PEI) gel system was larger than 500 Pa, which yet only induced a pressure gradient of 155.5 kPa/m, probably due to the brittleness of the gel (El-Karsani et al., 2015). In this study, the fast crosslinking gel system contributed to forming a double network gel. The loosely crosslinked weak gel has a large effect on the gel performances, which can reinforce the network of the tightly crosslinked gel (IMPG) (Xin et al., 2013; Krakovský et al., 2019). In addition, the toughness of the DN gel network may also be significantly improved, as shown in Fig. 4.

Moreover, the weak gel system and Na-MMT particles in the IMPG system endow the THSG gel a prominent thixotropy, which is beneficial for gel placement during the field application. In our previous work, the shear-thinning, hysteresis and buildup behavior of the gelant was systematically studied (Ge et al., 2022). It is found that the shear-thinning behavior is beneficial for the thixotropic gel to penetrate through the existing fractures with a relatively low injection pressure. The high viscous force of the thixotropic gelant would be favorable for filling the entire inclined fractures and plugging the whole fractures with gel. In this study, the preferred compositions of the THSG are 5 wt% AM, 0.05 wt% V501, 0.1 wt% MBA, 0.4 wt% PF, 0.2 wt% HPAM, 0.0125 wt% chromium acetate (Cr (III)), and 1.5 wt% Na-MMT.

#### 3.1.3. The effect of clay particles on gel properties

It should be noted that the performance of the THSG is largely determined by the clays used. There are many active groups on the

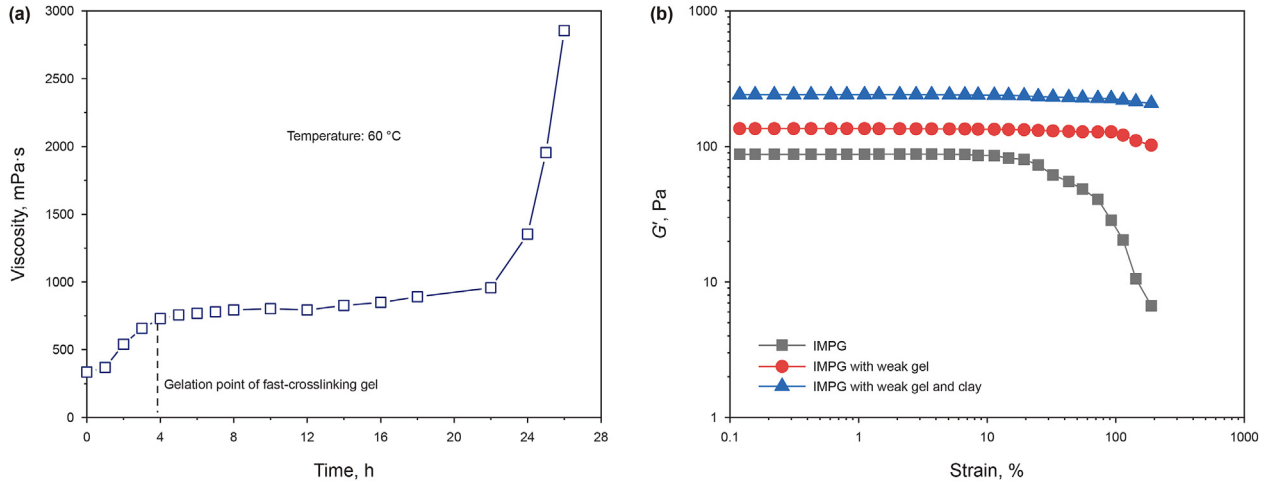


**Fig. 5.** Gel performances: (**a**) viscosity vs. time curve at a shear rate of 10 $s^{-1}$; (**b**) strength of gel samples with different components after being aged at 60 °C for 5 days.

surfaces and interlayers of clays, which can form firm structures with the chemical groups (hydroxyl, carboxyl, and aldehyde groups in polymers) by covalent bonding, surface grafting, and interlayer inserting (Filippone et al., 2008; Shibayama, 2011). Moreover, the hydrogen bonds between the clays and water can improve the ratio of the bound water. No syneresis was observed during the 12-month period in the presence of clays. However, the interactions between the clay particles and polymers would accelerate the formation of the network. Thus, the gelation time was shortened by addition of the Na-MMN, as illustrated in Fig. 3.

The dispersion of Na-MMT in the THSG was investigated by XRD and SEM measurements, and the results are shown in Fig. 6. The Na-MMT was pre-immersed in the IMPG solution, allowing the chemical components to absorb, permeate and insert into the interlayers of the clays. Fig. 6 shows that the angular locations of the peeks in the gelant and the gel samples were decreased to lower values, which indicated an increase in the interlayer spacing of the clays. Based on the peak angle and the Bragg's law, the interlayer spacing ($d$) of these samples was calculated, and the results are summarized in Table 4. The results show that the interlayer spacing of Na-MMT in the THSG solution was increased to 1.89 nm (compared to 1.74 nm in brine), which indicated that the gelant may be intercalated into the Na-MMT layers. The SEM photographs indicated that the gelant formed a stable network structure, and the Na-MMT was absorbed and inserted into the network structure. After gelation, the interplanar spacing of Na-MMT was increased to 2.12 nm. These results revealed that the crosslinking network was formed between the layers of Na-MMT, which led to an expansion

**Table 4**
The diffraction angle and the interplanar spacing of Na-MMT under different conditions.

| Samples | 2$\theta$, degree | $d$, nm |
|---|---|---|
| Na-MMT particles | 5.08 | 1.74 |
| THSG gel solution | 4.66 | 1.89 |
| THSG gel | 4.16 | 2.12 |

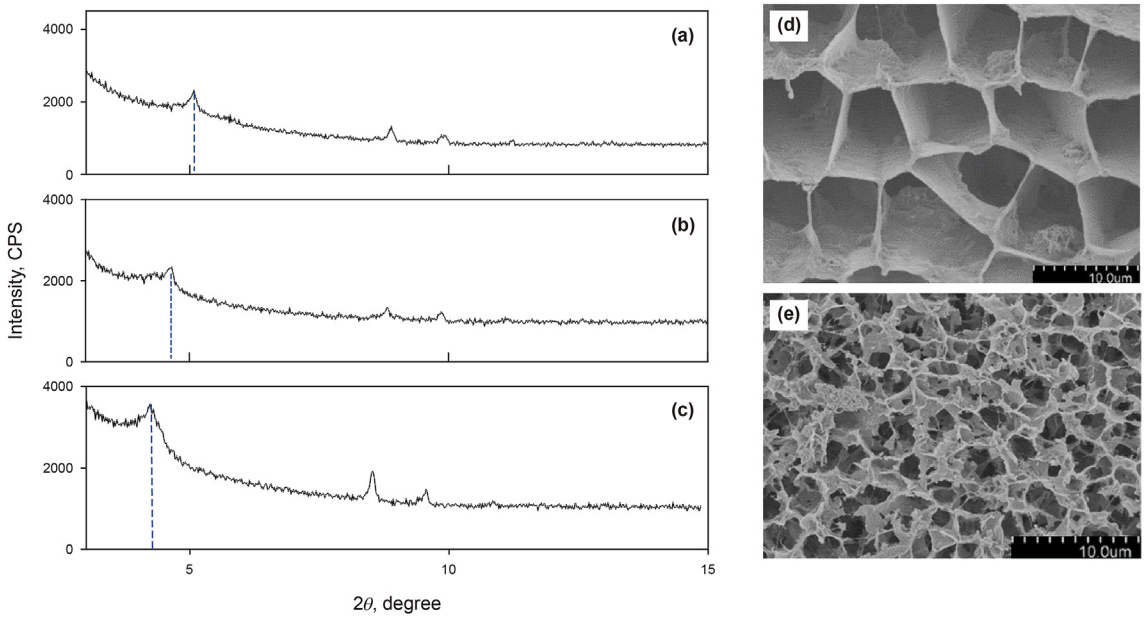


**Fig. 6.** XRD patterns of 8 wt% clay particles in 1/5 brine (**a**), gelant with 1.5 wt% clay (**b**), and gel with 1.5 wt% clay (**c**); SEM images of gelant (**d**) and gel (**d**).

of the Na-MMT layers. These micrographs indicated that the gel formed a firm and uniform network structure, which contributed to a high gel strength.

### 3.2. Swelling behavior of gels

The prepared gel samples were firstly immersed into brine with different salinity to observe if the gel would be swollen in different brine, and subsequently the gel strength was determined. Fig. 7a shows the effect of brine salinity on the gel swelling behavior. The results show that the gel sample soaked in fresh water exhibited the highest swelling ratio (more than 1000%) after equilibrium. Moreover, the gels soaked in brine of various salinity showed similar swelling behavior. The swelling ratio of gels soaked in different brine were approximately 400%. No shrinkage of the gel was observed even in the brine whose salinity was much higher than that used for preparing the gel solvent. The properties of the swollen gels are of particular importance to the gel blocking capacity during subsequent water floods. It was also found that the time needed for gel swelling was increased with increasing the brine salinity. This may be due to the low osmotic pressure difference between the high salinity brine and the gels.

In addition, the strength of the swollen gel was also measured, as shown in Fig. 7b. The results show that the gel strength (without swelling) was increased with aging time. The strength of the gel was more than 400 Pa after it had been aged for 180 days. For the swollen gels, the gel strength was initially increased in the first 30 days, after then it started to decrease. Although the gel immersed in fresh water showed a lower gel strength than those immersed in high salinity brine, it still demonstrated a relatively high strength and its $G'$ value was about 180 Pa after being soaked in the fresh water for 180 days. This is probably because the swelling of gel in water only expanded the volume of the gel and did not damage the crosslinking chains (Wang et al., 2012).

### 3.3. Rupture pressure

A successful gel treatment depends heavily on the gel plugging efficiency during chase water flooding. In order to systematically evaluate the blocking performance of the gel, the slim tubes with various diameters were used. In this study, the rupture pressure of gel is defined as the peak pressure during brine injection at which the gel was first breakthrough and the injected brine was flowing out from the outlet (Wilton and Asghari, 2007).

Fig. 8a shows the rupture pressure of the THSG as a function of the diameter of the gel-filled tubes. Several repeated experiments were conducted, and the major occurrences of rupture pressure are indicated by the box. The results show that the gel blocking capacity was decreased with increasing the diameter of the tube. When the gel was placed in a 1 mm tube, it required at least 19.2 MPa/m pressure gradient for brine to firstly break through the gel. In comparison, in a 4 mm diameter tube, the highest rupture pressure gradient was found to be 8.4 MPa/m. After gel rupture, brine was continuously injected and the injection pressure across the gel-filled tube was recorded. The salinity of injected brine was the same as that of the gel solvent. Fig. 8b shows the injection pressure was drastically fluctuated, and the injection pressure was even increased to a value that is higher than the gel rupture pressure. This phenomenon may be associated with the gel swelling behavior (Brattekås and Seright, 2018; Brattekås et al., 2016). After a period of fluctuations, the pressure levelled off and kept relatively stable at 1.65 MPa for a long period.

The swelling tests have shown that the THSG has a high swelling ratio, and the gel still has a high strength after swelling. To further investigate the effect of the injection brine salinity on the gel blocking ability, two injection scenarios were applied. In the first injection scenario, a high-salinity brine was injected after injection of the freshwater, while in the second scenario, the high-salinity brine was injected before the freshwater. The injected water was changed after the pressure across the gel-filled tube was stable. The rupture pressure of the gel measured by different brine was about 6.5 MPa, indicating that the initial salinity of brine had insignificant impacts on the gel rupture pressure. This is mainly due to the fairly short time needed for brine breakthrough the gel-filled tube at the point of gel rupture.

However, the pressure during continuous water flooding is largely dependent on the brine salinity. It can be seen from Fig. 9a that during freshwater flood the injection pressure was even temporarily higher than the gel rupture pressure. After the gel was ruptured, water started to flow through the narrow paths, which caused a significant swelling of the gel. The swollen gel would reblock the flow pathway during chase floods. At the peak pressure point, part of the gel was even squeezed out from the tube. After 400 tube volume (TV) of freshwater flooding, the pressure leveled off and the value was approximately 1.7 MPa. Then, brine was injected. The injection pressure was observed to be continuously

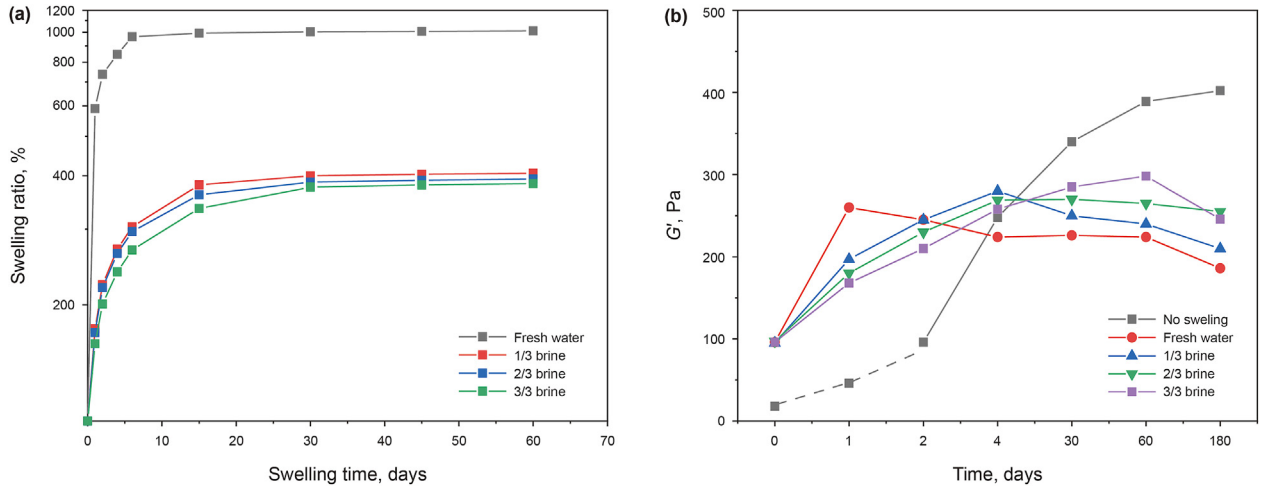


**Fig. 7.** Swelling behavior of gel in brine: (**a**) swelling ratio; (**b**) strength. The strength of soaked gel at the first point (0 day) was the initial strength of the gel after being aged at 60 °C for 2 days. The first black point is the strength of the gelant, and the second one is the strength of gel after semi-gelation.

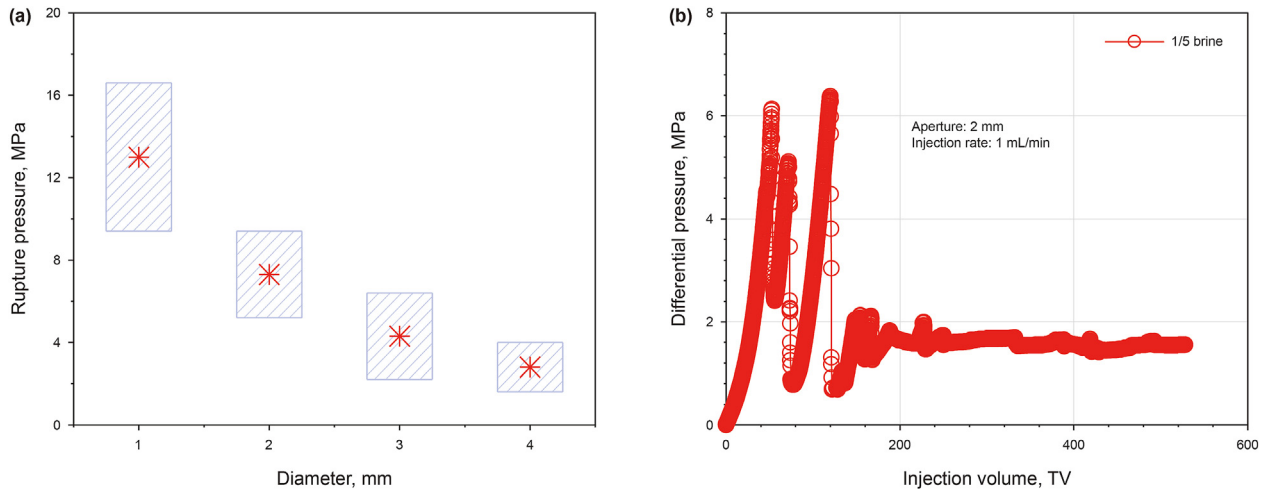


**Fig. 8.** Blocking ability of THSG. (**a**) Rupture pressure of THSG in tubes of different diameters. Six repeated experiments were performed, and the major results were shown in the box; the red asterisk is the average rupture pressure. (**b**) Differential pressure during continuous water injection. The composition of the injected brine is the same as that of the gel solvent.

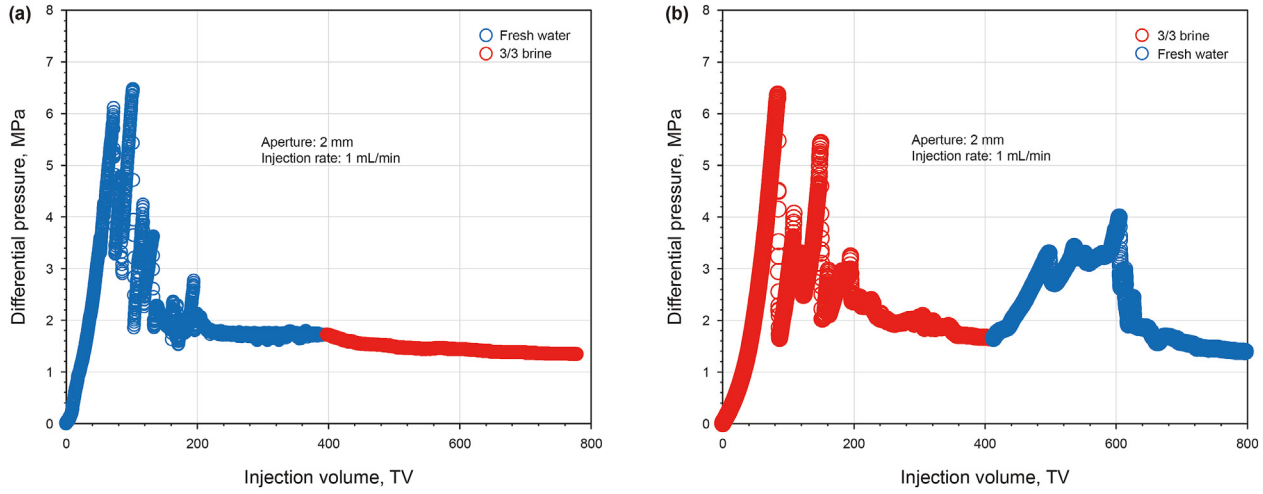


**Fig. 9.** The effect of water salinity on blocking capacity of gel in 2 mm tubes: (**a**) high-salinity brine after freshwater; (**b**) first high-salinity brine then freshwater.

decreased, possibly due to a shrinkage of the highly-swollen gel during brine injection. For the second injection scenario, completely different results were observed. As shown in Fig. 9b, the injection pressure was increased immediately, when freshwater flooding was begun. The results demonstrate that the swollen gel in the tube exhibited an improved blocking ability. Moreover, the high rupture pressure of the THSG gel would contribute to an effective gel treatment in large aperture fractures.

### 3.4. Propagation behavior of gelant in fractured cores

#### 3.4.1. Effect of matrix permeability on gelant propagation

Three different fractured cores (M-1, M-2, and M-3) were used to investigate the effect of the matrix permeability on gelant propagation. The fracture apertures were fixed at 2 mm, and the injection rate was 1 mL/min. The pressure gradients as a function of the volume of gelant injected (in terms of the volume of fractures, FV) were shown in Fig. 10. The pressure gradient increased rapidly at the initial stage of gelant injection and then increased slowly after 1 FV. After the fracture was filled with the gelant (1 FV), the pressure gradient in core M-1 was leveled off with a relatively low pressure gradient (6 kPa/m), which is lower than a commonly accepted pressure gradient in the field (22.6 kPa/m or equivalently, 1 psi/ft). The shear-thinning behavior of the gelant may contribute to the low injection pressure. It is reported in several studies that, at a fixed injection rate, the gel would propagate through a fracture in a stable way, and the permeability of the matrix has litter effect on the gel injection pressure (Seright, 2001; Sydansk et al., 2004; Bai et al., 2015; Seright and Brattekås, 2021). Whereas, in this study, the injection pressure was constantly increased with a slow rate during continuous gelant injection. It is hypothesized that the increase in the injection pressure was resulted from a formation of the filter cake on the fracture face. Since the fast-crosslinking gel system and Na-MMT can form a weak network structure (as shown in Fig. 6d), the formation of a weak gel filter cake during THSG injection may be largely facilitated. Moreover, a fast formation of the gel filter cake on the fracture surface can limit the leakoff of THSG compositions into the matrix.

The picture in the upper left of Fig. 10 shows that a gel filter cake was clearly formed on the fracture face, which would further reduce the effective aperture of the fracture and consequently lead to an increase in the gelant injection pressure. Moreover, it is

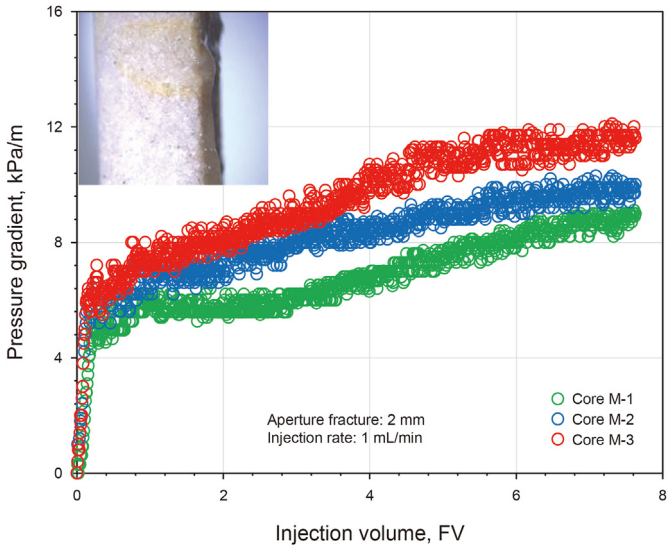


**Fig. 10.** Pressure gradient versus volume of gelant injected for core samples with different matrix permeability.

observed that the trend of pressure increase was more pronounced if the matrix permeability is higher. For core M-2, the pressure gradient was increased from 7 to 10 kPa/m during 6 FV gelant injection (1-7 FV). For core M-3, the pressure gradient was increased continuously to 12 kPa/m after 5 FV gelant injection (1-6 FV), before being leveled-off after approximately 6 FV. The fracture connected to higher permeability matrix has a rougher fracture surface. It may be easier for the fast-crosslinking gel to be adhered onto the rougher surface, consequently limiting the gelant leakoff. Thus, a high permeability matrix adjacent to the fracture may promote the formation of the gel filter cake.

After gel treatment, the matrix damage was evaluated. The results are summarized in Table 5. The permeability damage ratios for cores M-1, M-2, M-3 were 13.6%, 9.5%, and 10.2%, respectively. The results show that the core samples with a higher matrix permeability (M-2 and M-3) exhibited relatively smaller matrix damage. The result is consistent with the discussion above that a fast formation of the gel filter cake on the fracture face would reduce the extent of matrix permeability damage.

### 3.4.2. Effect of aperture fracture on gel treatment

Fig. 11 shows the effect of aperture size on gelant injection pressure and the matrix permeability reduction after gel placement. The results show that the gelant injection pressure gradient was significantly increased as the aperture size was decreased. At an injection rate of 1 mL/min, the pressure gradient was 20 kPa/m in a 0.5 mm fracture, compared to 4 kPa/m in a 3 mm aperture after 1 FV of the gelant injection. Furthermore, the results showed that the pressure drop was increased significantly in a smaller aperture during continuous gelant injection. However, the pressure gradient did not increase much in 3 mm fracture aperture during continuous gelant injection. The continuously increased pressure drop in a smaller aperture might be due to the rapid formation of the gel filter cake on the fracture face, causing a reduction of the effective size of the aperture.

**Table 5**
Matrix permeability damage after gel treatment.

| Core No. | $k_i$, mD | $k_d$, mD | $R_m$, % |
|---|---|---|---|
| 1 | 11 | 9.5 | 13.6 |
| 2 | 84 | 76 | 9.5 |
| 3 | 1860 | 1670 | 10.2 |

The permeability reduction ratios of the matrix after gel treatment are illustrated in Fig. 11b. The matrix damage ratios for cores A-1, A-2, A-3 and A-4 were 6.5%, 7%, 9.5% and 7.8%, respectively. The results indicated that a rapid formation of the gel filer cake in small aperture could result in low matrix damage. However, for core A-4 (with the largest aperture fracture), a relatively low matrix damage ratio was observed, which may be probably because the low injection pressure limited the leakoff of the gelant into the matrix (Bai et al., 2021). Thus, it can be concluded that a smaller aperture may lead to a more rapid formation of the gel filter cake, which might reduce the extent of matrix damage.

### 3.4.3. Effect of injection rate on gel treatment

Fig. 12 illustrates the effect of injection rate on the gelant injection pressure and matrix permeability reduction in 2 mm aperture fractures. The results show that the injection pressure was significant increased with increasing the injection rate. For example, at an injection rate of 4 mL/min, the pressure gradient reached 32 kPa/m, and then was gradually increased during continuous gelant injection. At 1 mL/min, the pressure gradient was as high as 7 kPa/m and then slightly increased as more gelant was injected. It can be concluded from the above discussion that the increase in injection pressure was a result of the formation of the gel filter cake on the fracture face, and the formation of gel filter cake can reduce the effective aperture size. Moreover, a more rapid increase in the injection pressure implied a faster formation of the gel filter cake. It also can be observed from Fig. 12a that a higher injection rate may lead to a faster formation of the gel filter cake.

The matrix permeability of the fractured cores (I-1, I-2, and I-3) was measured after the gel treatments. Fig. 12b illustrates the matrix permeability before and after the gel treatment. The matrix damage ratios were 9.5%, 8.2% and 11.4%, when the injection rates were 1, 2, and 4 mL/min, respectively. The results showed that the advantage of a fast gel filter cake formation at a high injection rate was not such significant, which may be nullified by the simultaneously high injection pressure at a higher flow rate. At an injection rate of 4 mL/min, some gelant may be initially leaked into the matrix even before the gel filter cake was formed, resulting in a high matrix damage ratio.

## 3.5. Blocking ability of gel in fractures

The effect of matrix permeability on gel blocking ability was studied. The pressure across the fractured core was measured as a function of the brine injected. Fig. 13 illustrates the pressure gradients of fractured cores with different matrix permeability. The peek pressure gradients for the fractured cores M-1, M-2 and M-3 were 4.2, 0.39, and 0.05 MPa/m, respectively. After several PV of brine injection, the injection pressure was almost stable. It should be noted that the pressure gradients would be 3.6, 0.37, and 0.03 MPa/m (1 mL/min), if core samples M-1, M-2 and M-3 were not fractured. Moreover, due to the viscoelasticity and swelling behavior of the gel, the injection pressure would be fluctuated when brine flows through the gel-filled fractures. Thus, it is hypothesized that most of the injected brine may be diverted into the matrix, and the fracture may be completely blocked by the THSG gel. The injection pressure for the fractured core after gel treatment was still moderately higher than that for the matrix, which is probably due to the formation of gel at the inlet and outlet of the core faces, as shown in the pictures underneath Fig. 13.

The magnitude of the permeability reduction for fractured core was extremely high, even after experiencing long periods of brine flooding. After 12 PV of brine had been injected, the water residual

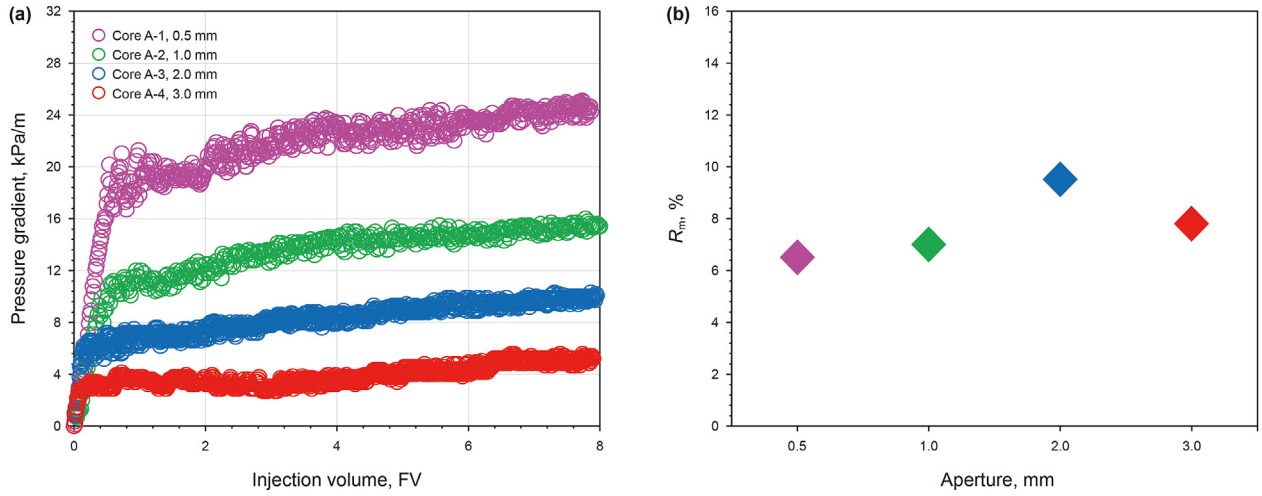


**Fig. 11.** Gelant propagation in different aperture fractures: (**a**) pressure gradient versus volume of gelant injected; (**b**) matrix permeability reduction ratios after gel treatment.

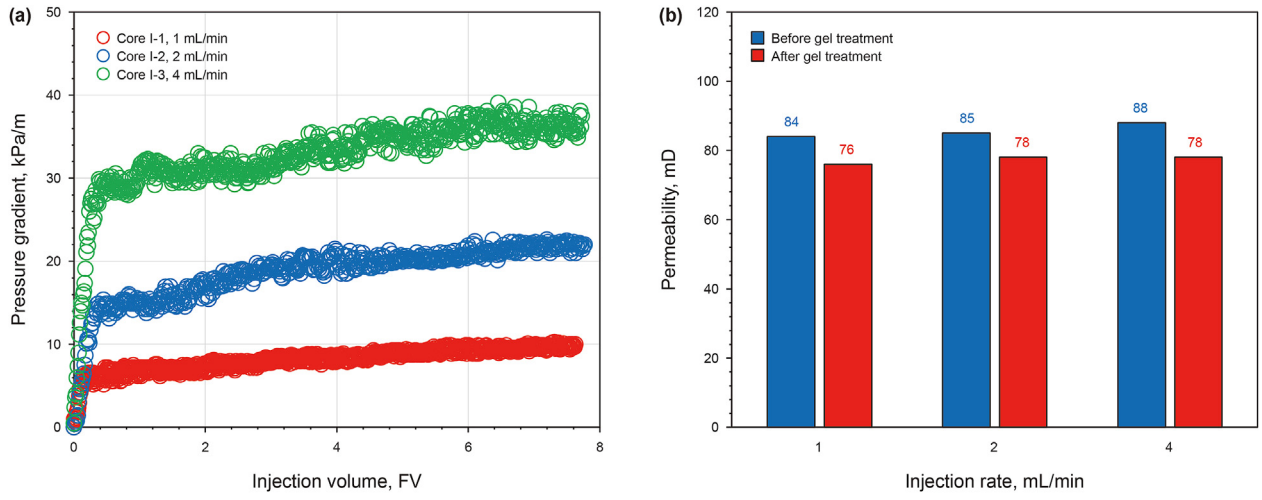


**Fig. 12.** The effect of injection rate on gelant propagation: (**a**) pressure gradient versus volume of gelant injected; (**b**) matrix permeability reduction ratio after gel treatment.

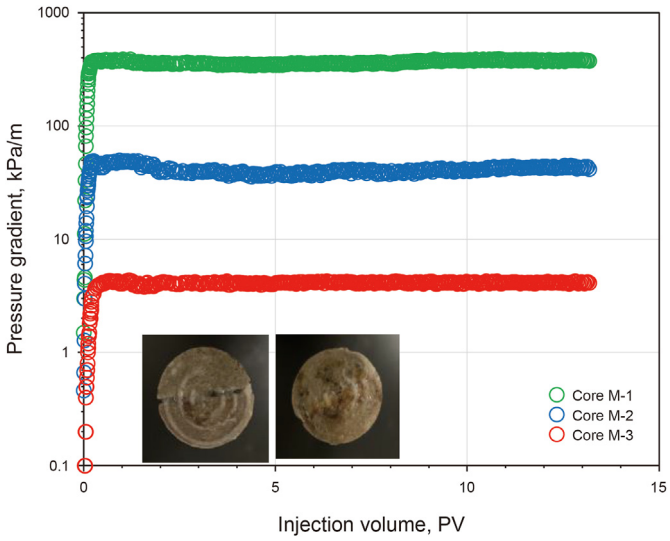


**Fig. 13.** Blocking ability of gel in fractured cores with different matrix permeability. After gelant injection, the fractured cores M-1, M-2, and M-3 were aged at 60 °C for 3 days before blocking ability tests.

resistance factor ($F_{rrw}$) for cores M-1, M-2 and M-3 was about 97,000, 8,740 and 1,150, respectively. The results show that the values of $F_{rrw}$ were significant increased with decreasing the matrix permeability. The result is consistent with that reported by Seright (2009), who pointed out that the fractures were less likely to be channeled through by brine if the matrix permeability was higher. Bai et al. (2015) also reported that the polymer gel demonstrated better performance for water shutoff in fractured core when the matrix permeability was higher. For a fractured core with high matrix permeability, the gel would more likely resist a relatively low-pressure gradient during chase brine flooding. Thus, for a fractured core with lower matrix permeability, the gel should provide a higher residual resistance factor to achieve a desirable gel performance. It should be noted that the injection rate and aperture fracture have almost no effect on the gel blocking ability for gel treatment in Berea sandstone of similar matrix permeability. This might be because the fractures were completely blocked by the gel, and the injected water could only pass through the matrix. Therefore, the flow behaviors are similar.

### 3.6. Enhanced oil recovery test

Cores O-1 and O-2 were used for core flooding tests to determine the oil recovery and evaluate the wormhole formed by oil or water. Initially, the cores were directly saturated with oil under vacuum. After water flooding (WF), a certain amount of gelant was injected (GI) into the fractured cores, then the core samples were shut-in such that gel can be readily formed. After then, chase brine was injected to evaluate the effectiveness of gel on improved oil recovery. As discussed above, the THSG can withstand a high-pressure gradient in the fracture, and the fracture could be completely blocked by the THSG gel. In order to evaluate the effect of gel swelling on oil recovery factor, the gelant in core O-2 was only aged for 30 h. In this case, the gel was not maturely formed in the fractures.

The oil recovery factor, oil cut, and injection pressure at different stages are shown in Fig. 14. The fluid injection rates during fractured core test were kept constant at 1 mL/min. In these core flooding tests, it is assumed that the oil in the fractures was firstly swept. Therefore, the oil recovery factor by initial waterflooding, gelant injection and the chase waterflooding were all based on the amount of oil in the matrix in this study. The results show that the oil recovery factor during the first stage of water flooding for cores O-1 and O-2 was only 1.2% and 0.9%, respectively. Moreover, the incremental oil recovery was 7.6% and 7.8%, respectively, for cores O-1 and O-2 during the gelant injection. From the oil cut, it can be seen that certain amount of oil was produced during injection of the first FV of the gelant. The results indicate that the oil recovery during gelant placement was limited. It was claimed that the viscous effect of the gel was relatively small compared to the plugging effect for gel treatments in a fractured porous media (Alshehri et al., 2018).

For core O-1, the oil recovery was improved by 65.3% (with 2 PV of brine) after the gel treatment. The peak pressure gradient was approximately 467 kPa/m, and the pressure gradient was finally stable at 400 kPa/m. No water path was detected in the gel-filled fracture after the used core was split. As shown in Fig. 15b, only some oil-wormholes were found in the gel. For core O-2, the gel in the fracture was not completely gelated due to the short aging time, therefore, the gel exhibited a relatively low strength. During the chase waterflooding, it is found that the injected brine could break through from the gel-filled fracture. A noteworthy peak pressure was obtained before the injection pressure was significantly decreased. The oil recovery factor was improved by 40.2% after 4 PV of chase water flooding. It can be clearly seen that water flow paths were formed along the copper wire after splitting core O-2 (Fig. 15c). However, the pathway was still much narrower than the aperture fracture. Therefore, the ruptured gel in the fracture still has a high resistant factor to brine, and consequently the oil cut was still higher than 10% after injecting 2 PV of brine. However, the incremental oil recovery factor for core O-2 was small compared to that of core O-1 (in which the fracture was completely blocked).

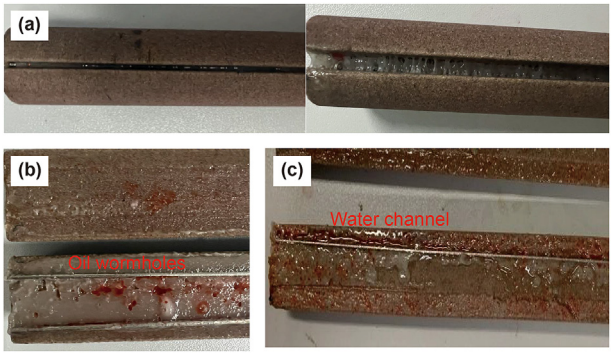


**Fig. 15.** Fractured core after gel treatment: (**a**) separating the fractured core; (**b**) core O-1: oil-wormholes were formed by oil, no water flowed through the gel-blocked fracture; (**c**) core O-2: water channels were formed in the gel treated fracture, but the fractured core still had a high oil recovery after gel rupture. The model oil has been colored to red in the experiments.

After no oil was produced from core O-2 during chase brine flooding, freshwater was injected. As shown in Fig. 16, the injection pressure was gradually increased and water cut was decreased at the initial stage, when freshwater started to be injected. The incremental oil recovery factor during freshwater injection was 7.1%, which may be due to the improvement in the sweep efficiency or (and) displacement efficiency. 8 PV of freshwater was also injected into core O-1 after the chase water, and the oil recovery factor was increased by 6.5%. The results show that the incremental oil recovery factor by fresh water for core O-1 was comparable to that of core O-2, implying that the improved blocking ability by the swollen gel has little effect on the sweep efficiency improvement.

## 4. Conclusions

Gel treatment is one of the most successful applications for water-shutoff in fractured reservoirs, and its efficiency could be

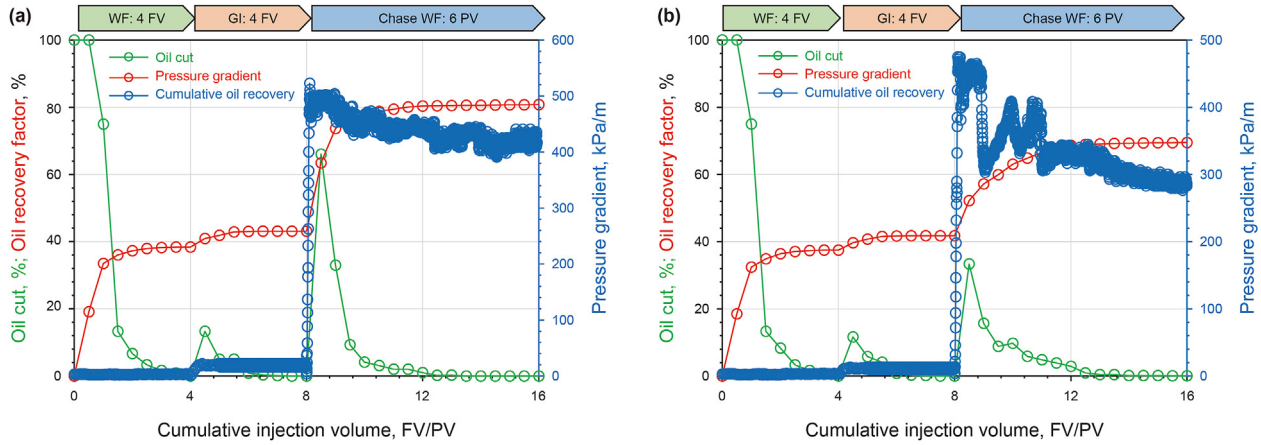


**Fig. 14.** Oil cut, oil recovery factor, and injection pressure gradient for different period flooding: (**a**) core O-1 aged for 3 days, and the fracture was completely blocked by gel; (**b**) core O-2 aged for 30 h.

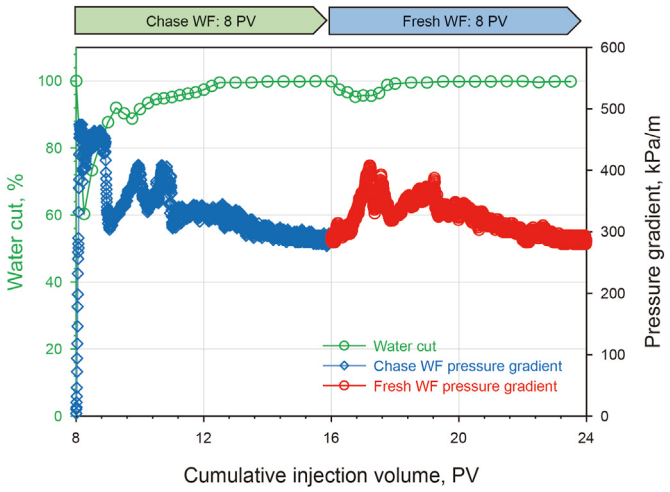


**Fig. 16.** Pressure gradient and water cut during chase flooding after gel treatment in core O-2.

largely benefited from using a double network gel. The THSG was formulated with two highly asymmetrically crosslinked network: a tightly crosslinked network by monomer polymerization to build the high-strength gel, and a loosely crosslinked network by fast-crosslinked polymer gels to strengthen the first gel network and mitigate the gelant leakoff. The THSG is quite robust and can be tailored to a wide range of reservoir conditions, with programmable gelation time, high gel strength, remarkable thermal stability, and excellent swelling behavior. The merits of THSG for gel treatment in fractures were verified by the rupture pressure tests and core flooding tests. The main conclusions and findings of this study are listed in the following.

(1) The double network of THSG endowed the gel a high rupture pressure in tubes of various diameters. After the gel was ruptured, a swelling of the gel would significantly improve the gel blocking ability. The improvement was more pronounced during low-salinity brine injection.
(2) A low injection pressure gradient was observed during the gelant injection. The fast-crosslinking of the polymer gel and Na-MMT resulted in a fast formation of the gel filter cake on the fracture face. Moreover, a high matrix permeability adjacent to the fracture would promote the formation of the gel filter cake. The matrix permeability damage may be mitigated by the formation of the gel filter cake on the fracture face.
(3) After the gel treatment, the fractures of the core were completely blocked by the THSG, diverting the subsequently injected brine into the matrix. The fractured cores exhibited a high residual resistance factor to water ($F_{rrw}$) after the gel treatment. For an effective gel treatment, the desired value of $F_{rrw}$ would be significantly increased with decreasing the matrix permeability. The results illustrated that a higher strength gel would be required for treatment in fractures connected to a lower permeability matrix.
(4) The swelling of the immature gel during chase water flooding (through the gel-filled fracture) can improve the oil recovery. Compared to the completely blocked fractures, however, the incremental oil recovery was less effective for the weak gel.
(5) Even though the blocking ability of the weak gel can be enhanced after being swollen in the presence of fresh water, its effectiveness on improving oil recovery is still less prominent compared to an improvement in sweep efficiency by injection of fresh water.

## Declaration of competing interest

The authors declare that they have no known competing financial interests or personal relationships that could have appeared to influence the work reported in this paper.

## Acknowledgments

The financial support from the Major Scientific and Technological Projects of CNPC under Grant (ZD2019-183-007) is gratefully acknowledge.

## References

Alhuraishawy, A.K., Bai, B., Imqam, A., Wei, M., 2018. Experimental study of combining low salinity water flooding and preformed particle gel to enhance oil recovery for fractured carbonate reservoirs. Fuel 214, 342–350. https://doi.org/10.1016/j.fuel.2017.10.060.
Al-Muntasheri, G.A., Nasr-El-Din, H.A., Zitha, P.L., 2008. Gelation kinetics and performance evaluation of an organically crosslinked gel at high temperature and pressure. SPE J. 13 (3), 337–345. https://doi.org/10.2118/104071-PA.
Alshehri, A.J., Wang, J., Kwak, H.T., AlSofi, A.M., 2018. A coreflooding-NMR study of gel conformance control in fractured systems. SPE Kingdom of Saudi Arabia Annual Technical Symposium and Exhibition. https://doi.org/10.2118/194383-MS.
Bai, Y., Wei, F., Xiong, C., Li, J., Jiang, R., Xu, H., Shu, Y., 2015. Effects of fracture and matrix on propagation behavior and water shut-off performance of a polymer gel. Energy Fuels 29 (9), 5534–5543. https://doi.org/10.1021/acs.energyfuels.5b01381.
Bai, Y., Zhang, Q., Sun, J., Shang, X., Lv, K., Wang, F., 2021. Disproportionate filtration behaviors of polymer/chromium gel used for fracture plugging. J. Mol. Liq. 343, 117567. https://doi.org/10.1016/j.molliq.2021.117567.
Brattekås, B., Seright, R.S., 2018. Implications for improved polymer gel conformance control during low-salinity chase-floods in fractured carbonates. J. Petrol. Sci. Eng. 163, 661–670. https://doi.org/10.1016/j.petrol.2017.10.033.
Brattekås, B., Graue, A., Seright, R.S., 2016. Low-salinity chase waterfloods improve performance of Cr (III)-acetate hydrolyzed polyacrylamide gel in fractured cores. SPE Reservoir Eval. Eng. 19 (2), 331–339. https://doi.org/10.2118/173749-PA.
Brattekås, B., Pedersen, S.G., Nistov, H.T., , Haugen, Å., Graue, A., Liang, J.-T., Seright, R.S., 2015. Washout of Cr(III)-acetate-HPAM gels from fractures: effect of gel state during placement. SPE Prod. Oper. 30, 99–109. https://doi.org/10.2118/169064-PA.
Canbolat, S., Parlaktuna, M., 2019. Polymer gel conformance on oil recovery in fractured medium: visualization and verification. J. Petrol. Sci. Eng. 182, 106289. https://doi.org/10.1016/j.petrol.2019.106289.
Chen, L., Zhu, X., Fu, M., Zhao, H., Li, G., Zuo, J., 2019. Experimental study of calcium-enhancing terpolymer hydrogel for improved oil recovery in ultrodeep carbonate reservoir. Colloids Surf. A Physicochem. Eng. Asp. 570, 251–259. https://doi.org/10.1016/j.colsurfa.2019.03.025.
Demir, M., Topguder, N.N.S., Yilmaz, M., Ince, Y., Karabakal, U., Gould, J.H., 2008. Water shutoff gels improved oil recovery in naturally fractured Raman heavy oilfield. In: SPE Russian Oil and Gas Technical Conference and Exhibition. https://doi.org/10.2118/116878-MS.
Du, D.J., Pu, W.F., Tan, X., Liu, R., 2019. Experimental study of secondary crosslinking core-shell hyperbranched associative polymer gel and its profile control performance in low-temperature fractured conglomerate reservoir. J. Petrol. Sci. Eng. 179, 912–920. https://doi.org/10.1016/j.petrol.2019.05.006.
El-Karsani, K.S., Al-Muntasheri, G.A., Sultan, A.S., Hussein, I.A., 2015. Gelation of a water-shutoff gel at high pressure and high temperature: rheological investigation. SPE J. 20 (5), 1103–1112. https://doi.org/10.2118/173185-PA.
Eoff, L., Funkhouser, G.P., Cowan, M., 2001. High-density monomer system for formation consolidation/water-shutoff applications. SPE Prod. Facil. 16 (3), 176–180. https://doi.org/10.2118/72996-PA.
Filippone, G., Dintcheva, N.T., Acierno, D., La Mantia, F.P., 2008. The role of organoclay in promoting co-continuous morphology in high-density poly (ethylene)/poly (amide) 6 blends. Polymer 49 (5), 1312–1322. https://doi.org/10.1016/j.polymer.2008.01.045.
Ganguly, S., Willhite, D.P., Green, D.W., McCool, C.s., 2002. The effect of fluid leakoff on the gel placement and gel stability in fractures. SPE J. 7 (3), 309–315. https://doi.org/10.2118/79402-PA.
Ge, J., Wu, Q., Ding, L., Guo, H., Zhao, A., 2022. Preparation and rheological Evaluation of a thixotropic polymer gel for water shutoff in fractured tight reservoirs. J. Petrol. Sci. Eng. 208, 109542. https://doi.org/10.1016/j.petrol.2021.109542.
Gong, J.P., 2010. Why are double network hydrogels so tough? Soft Matter 6 (12), 2583–2590. https://doi.org/10.1039/B924290B.
Guo, H., Ge, J., Wu, Q., He, Z., Wang, W., Cao, G., 2022. Syneresis behavior of polymer

gels aged in different brines from gelants. Gels 8 (3), 166. https://doi.org/10.3390/gels8030166.
Haque, M.A., Kurokawa, T., Gong, J.P., 2012. Super tough double network hydrogels and their application as biomaterials. Polymer 53 (9), 1805–1822. https://doi.org/10.1016/j.polymer.2012.03.013.
Imqam, A., Bai, B.J., 2015. Optimizing the strength and size of preformed particle gels for better conformance control treatment. Fuel 148, 178–185. https://doi.org/10.1016/j.fuel.2015.01.022.
Jamali, A., Moghbeli, M.R., Ameli, F., Roayaie, E., Karambeigi, M.S., 2020. Synthesis and characterization of pH-sensitive poly (acrylamide-co-methylenebisacrylamide-co-acrylic acid) hydrogel microspheres containing silica nanoparticles: application in enhanced oil recovery processes. J. Appl. Polym. Sci. 137 (12), 48491. https://doi.org/10.1002/app.48491.
Jia, H., Pu, W.F., Zhao, J.Z., Liao, R., 2011. Experimental investigation of the novel phenol– formaldehyde cross-linking HPAM gel system: based on the secondary cross-linking method of organic cross-linkers and its gelation performance study after flowing through porous media. Energy Fuels 25 (2), 727–736. https://doi.org/10.1021/ef101334y.
Kang, W., Kang, X., Lashari, Z.A., Li, Z., Zhou, B., Yang, H., Sarsenbekuly, B., Aidarova, S., 2021. Progress of polymer gels for conformance control in oilfield. Adv. Colloid Interface Sci. 289, 102363. https://doi.org/10.1016/j.cis.2021.102363.
Khamees, T.K., Flori, R.E., 2018. A comprehensive evaluation of the parameters that affect the performance of in-situ gelation system. Fuel 225, 140–160. https://doi.org/10.1016/j.fuel.2018.03.115.
Krakovský, I., Kouřilová, H., Hrubovský, M., Labuta, J., Hanyková, L., 2019. Thermoresponsive double network hydrogels composed of poly (N-isopropylacrylamide) and polyacrylamide. Eur. Polym. J. 116, 415–424. https://doi.org/10.1016/j.eurpolymj.2019.04.032.
Lenji, M.A., Haghshenasfard, M., Sefti, M.V., Salehi, M.B., 2018. Experimental study of swelling and rheological behavior of preformed particle gel used in water shutoff treatment. J. Petrol. Sci. Eng. 169, 739–747. https://doi.org/10.1016/j.petrol.2018.06.029.
Lowe, A.B., McCormick, C.L., 2007. Reversible addition–fragmentation chain transfer (RAFT) radical polymerization and the synthesis of water-soluble (co) polymers under homogeneous conditions in organic and aqueous media. Prog. Polym. Sci. 32 (3), 283–351. https://doi.org/10.1016/j.progpolymsci.2006.11.003.
Mahon, R., Balogun, Y., Oluyemi, G., Njuguna, J., 2020. Swelling performance of sodium polyacrylate and poly (acrylamide-co-acrylic acid) potassium salt. SN Appl. Sci. 2 (1), 1–15. https://doi.org/10.1007/s42452-019-1874-5.
Seright, R., Brattekås, B., 2021. Water shutoff and conformance improvement: an introduction. Petrol. Sci. 18 (2), 450–478. https://doi.org/10.1007/s12182-021-00546-1.
Seright, R.S., 2001. Gel propagation through fractures. SPE Prod. Facil. 16 (4), 225–231. https://doi.org/10.2118/74602-PA.
Seright, R.S., 2003. An alternative view of filter-cake formation in fractures inspired by Cr(III)-acetate-HPAM gel extrusion. SPE Prod. Facil. 18 (1), 65–72. https://doi.org/10.2118/81829-PA.
Seright, R.S., 2009. Disproportionate permeability reduction with pore-filling gels. SPE J. 14 (1), 5–13. https://doi.org/10.2118/99443-PA.
Shibayama, M., 2011. Small-angle neutron scattering on polymer gels: phase behavior, inhomogeneities and deformation mechanisms. Polym. J. 43 (1), 18–34. https://doi.org/10.1038/pj.2010.110.
Sydansk, R.D., Al-Dhafeeri, A.M., Xiong, Y., Seright, R.S., 2004. Polymer gels formulated with a combination of high-and low-molecular-weight polymers provide improved performance for water-shutoff treatments of fractured production wells. SPE Prod. Facil. 19 (4), 229–236. https://doi.org/10.2118/89402-PA.
Sydansk, R.D., Xiong, Y., Al-Dhafeeri, A.M., Schrader, R.J., Seright, R.S., 2005. Characterization of partially formed polymer gels for application to fractured production wells for water-shutoff purposes. SPE Prod. Facil. 20 (3), 240–249. https://doi.org/10.2118/89401-PA.
Tu, T.N., Wisup, B., 2011. Investigating the effect of polymer gels swelling phenomenon under reservoir conditions on polymer conformance control process. Int. Petroleum Technol. Confer. https://doi.org/10.2523/IPTC-14673-MS.
Wang, J., AlSofi, A.M., AlBoqmi, A.M., 2016. Development and evaluation of gel-based conformance control for a high salinity and high temperature carbonate. In: SPE EOR Conference at Oil and Gas West Asia. https://doi.org/10.2118/179796-MS.
Wang, T., Liu, D., Lian, C., Zheng, S., Liu, X., Tong, Z., 2012. Large deformation behavior and effective network chain density of swollen poly (N-isopropylacrylamide)–laponite nanocomposite hydrogels. Soft Matter 8 (3), 774–783. https://doi.org/10.1039/C1SM06484C.
Wilton, R., Asghari, K., 2007. Improving gel performance in fractures: chromium pre-flush and overload. J. Can. Pet. Technol. (2), 33–39. https://doi.org/10.2118/07-02-04.
Wu, Q., Ge, J., Ding, L., Guo, H., Wang, W., Fan, J., 2022. Insights into the key aspects influencing the rheological properties of polymer gel for water shutoff in fractured reservoirs. Colloids Surf. A Physicochem. Eng. Asp. 634, 127963. https://doi.org/10.1016/j.colsurfa.2021.127963.
Wu, Q., Ge, J., Ding, L., Wei, K., Liu, Y., Deng, X., 2021. A successful field application of polymer gel for water shutoff in a fractured tight sandstone reservoir. In: SPE Middle East Oil & Gas Show and Conference. https://doi.org/10.2118/204741-MS.
Xin, H., Saricilar, S.Z., Brown, H.R., Whitten, P.G., Spinks, G.M., 2013. Effect of first network topology on the toughness of double network hydrogels. Macromolecules 46 (16), 6613–6620. https://doi.org/10.1021/ma400892g.
Yang, Y., Qiu, S., Xie, X., Wang, X., Li, R.K.Y., 2010. A facile, green, and tunable method to functionalize carbon nanotubes with water-soluble azo initiators by one-step free radical addition. Appl. Surf. Sci. 256 (10), 3286–3292. https://doi.org/10.1016/j.apsusc.2009.12.020.
Zhang, H., Bai, B., 2011. Preformed-particle-gel transport through open fractures and its effect on water flow. SPE J. 16 (2), 388–400. https://doi.org/10.2118/129908-PA.
Zhang, L., Yu, W., Ma, P., Zheng, L., Zhang, Y., 2021. Study on long-term rheological characteristics of polymer gel and prediction of its creep fracture time. J. Petrol. Sci. Eng. 201, 108445. https://doi.org/10.1016/j.petrol.2021.108445.
Zhang, X., Guo, X., Yang, S., Tan, S., Li, X., Dai, H., Yu, X., Zhang, X., Weng, N., Jian, B., Xu, J., 2009. Double-network hydrogel with high mechanical strength prepared from two biocompatible polymers. J. Appl. Polym. Sci. 112 (5), 3063–3070. https://doi.org/10.1002/app.29572.